How the dynamics of attachment to the substrate influence stress in metal halide perovskites

Gabriel R. McAndrews ; Boyu Guo ; Daniel A. Morales ; Aram Amassian ; Michael D. McGehee

Check for updates

View Online

Export Citation

AIP Publishing

How the dynamics of attachment to the substrate influence stress in metal halide perovskites

View Online   Export Citation   CrossMark

Gabriel R. McAndrews,[1] (iD) Boyu Guo,[2] (iD) Daniel A. Morales,[1] (iD) Aram Amassian,[2,a] (iD)
and Michael D. McGehee[1,3,4,a] (iD)

AFFILIATIONS

[1] Materials Science and Engineering Program, University of Colorado Boulder, 4001 Discovery Drive, Boulder, Colorado 80303, USA
[2] Department of Materials Science and Engineering, North Carolina State University, 911 Partners Way, Room 3002, Engineering Building I, Raleigh, North Carolina 27695, USA
[3] Renewable and Sustainable Energy Institute (RASEI), University of Colorado Boulder, 4001 Discovery Drive, Boulder, Colorado 80303, USA
[4] Department of Chemical and Biological Engineering, University of Colorado Boulder, Boulder, Colorado 80303, USA

[a] Authors to whom correspondence should be addressed: michael.mcgehee@colorado.edu
and aamassi@ncsu.edu

ABSTRACT

Metal halide perovskites have the potential to contribute to renewable energy needs as a high efficiency, low-cost alternative for photovoltaics. Initial power conversion efficiencies are superb, but improvements to the operational stability of perovskites are needed to enable extensive deployment. Mechanical stress is an important, but often misunderstood factor impacting chemical degradation and reliability during thermal cycling of perovskites. In this manuscript, we find that a commonly used equation based on the coefficient of thermal expansion (CTE) mismatch between perovskite and substrate fails to accurately predict residual stress following solution-based film formation. For example, despite similar CTEs there is a 60 MPa stress difference between narrow bandgap "SnPb perovskite" $Cs_{0.25}FA_{0.75}Sn_{0.5}Pb_{0.5}I_3$ and "triple cation perovskite" $Cs_{0.05}MA_{0.16}FA_{0.79}Pb(I_{0.83}Br_{0.17})_3$. A combination of *in situ* absorbance and substrate curvature measurements are used to demonstrate that partial attachment prior to the anneal can reduce residual stress and explain wide stress variations in perovskites.

I. INTRODUCTION

Metal halide perovskites, hereon referred to as perovskites for simplicity, are a promising class of semiconductors eagerly researched for use in solar cells. Single junction perovskite power conversion efficiencies (PCEs) have eclipsed 26%, which is nearing record silicon cell efficiencies, with room for improvement before theoretical limits are reached.[1,2] In addition, bandgap tunability has enabled perovskite–silicon tandems with independently certified PCEs of 33.7%.[3] Despite competitive PCEs, photovoltaics based on perovskites have not yet been deployed due to instability. The decomposition of perovskites to non-photoactive phases, such as yellow PbI_2, is driven and accelerated by environmental stressors, such as light, heat, moisture, and oxygen.[4–6] The avoidance of weakly

bonded and volatile organic cations, such as MA^+, and the use of moisture and oxygen blocking layers have been shown to be successful strategies to suppress phase instability.[7,8] Recent strides have been made to extend the operational lifetime of perovskites to above five years, but additional improvements would make the case for widespread use of perovskite photovoltaics.[9]

Strain engineering is important for improving phase stability and increasing energetic barriers to limit mobility of organic cations and halide species. While there are some exceptions, tensile strain has been shown to increase the rate of decomposition of perovskites.[10,11] In addition, tension is also linked to accelerated halide segregation, which is a key source of open circuit voltage loss.[12,13] The formation of perovskite thin films using solution processing methods usually includes a thermal annealing step to fully

20 April 2024 02:09:59

convert the film from intermediate to perovskite phases. Therefore, the field has primarily focused on thermal strain originating from a coefficient of thermal expansion (CTE) mismatch between perovskite and substrate.[10] Perovskites have an order of magnitude higher coefficients of thermal expansion (CTE) than substrates used for photovoltaic applications, such as silicon and glass.[14] Consequently, tensile strain and corresponding stress are predicted to develop in the perovskite layer while cooling back to room temperature due to the film's constraint to the substrate and inability to fully contract. To avoid the development of tensile stress, several strategies have been employed: selecting substrates with similar CTEs to the perovskite (such as polymers), lowering the film formation temperature, and using of additives in the precursor solution or antisolvent.[10,15] It is important to note that the stress mentioned in this work refers to a macro-stress that extends globally across the film rather than micro-stress, which refers to local structural and chemical disorder.[16,17]

In addition to the implications of stress on chemical degradation, excessive stress can result in mechanical failure, especially at low temperatures where the stress is even higher. Perovskites are inherently brittle, with cohesion energies an order of magnitude lower than that of silicon.[18,19] Without toughening strategies, they are susceptible to fracture and delamination, which can severely hinder photovoltaic performance and stability.[20–22] Other studies have demonstrated the importance of managing stress to improve perovskite thermomechanical stability.[15,22,23] For additional context, readers are directed to several reviews that emphasize the importance of reducing mechanical stress in perovskite thin films.[24–27]

In this work, we show that the CTE mismatch between perovskite and substrate can be a key source of thermal strain, but that the residual strain after film formation in perovskites is more complex. We clarify that the definition of attachment to the substrate is not equivalent to complete film formation and present evidence that the perovskite film can be attached to the substrate prior to the anneal. Next, we provide the evidence for this partial attachment model with *in situ* stress measurements during the anneal and subsequent cooldown. In addition, we show that conversion to the α-phase does not guarantee permanent attachment to the substrate. We suggest that the complex and dynamic nature of mechanical attachment observed in this work can explain the widely varying stresses reported in perovskite literature.

II. RESULTS AND DISCUSSION

A. Strain, stress, and Young's modulus measurements of thin film perovskites

While several methods to quantify stress or strain in perovskites have been reported, not all of them are reliable. X-ray diffraction (XRD) is a common, nondestructive method used to measure structural deformation, referred to as strain (ε), in perovskites. We did not use a single low-angle peak shift to calculate strain as other factors, such as slight compositional or alignment differences, can influence results. Instead, we used the more rigorous XRD:$\sin^2\psi$ method, which interrogates the shift of a higher angle diffraction peak at various sample tilts to probe the in-plane and out-of-plane lattice spacings.[28,29] This method is routinely used to quantify strain in crystalline or polycrystalline materials,[30,31] including

thin film perovskites.[32] With the $\sin^2\psi$ method, the strain is directly measured,

$$\varepsilon_f = \left(\frac{1 - \nu_f}{1 + \nu_f}\right)\frac{m}{d_0}, \tag{1}$$

where ν_f is the perovskite Poisson ratio ($\approx$0.30–0.33),[33,34] m is the fitted slope of the d-spacing vs $\sin^2\psi$, and d_0 is the strain-free lattice parameter approximated to be $d_{\psi=0}$ (supplementary material, Note 1, Fig. S1). Given the in-plane constraint of the perovskite film and assumed zero stress in the out-of-plane direction, the plane stress condition can be used to describe the relationship between stress (σ) and strain as[17]

$$\sigma_f = \frac{E_f}{1 - \nu_f}\varepsilon_f, \tag{2}$$

where E_f is the perovskite's Young's modulus.

The reported values for the Young's moduli of metal halide perovskites vary, and there are concerns that the nanoindentation method results in values that are higher than those obtained with other methods.[35] To avoid uncertainty in stress due to inaccurate Young's moduli, the stress in a thin film on a thick substrate can be directly measured by monitoring substrate curvature changes during processing (i.e., before and after film annealing) in accordance with the Stoney equation[36]

$$\sigma_f = \left(\frac{E_s}{1 - \nu_s}\right)\frac{t_s^2}{6t_f}\Delta\kappa. \tag{3}$$

E_s is the substrate Young's modulus, ν_s is the substrate Poisson ratio, t_s is the substrate thickness, t_f is the perovskite film thickness, and $\Delta\kappa$ is the change in substrate curvature. It is worth mentioning that the substrate curvature method requires relatively thin substrates to resolve changes in curvature and that the curvature must be measured before and after film casting. Stress reported with curvature represents a global average and unraveling any depth dependent stress gradients is better suited to the XRD:$\sin^2\psi$ method.[37]

The substrate curvature can be determined by mapping the surface profile with a stylus profilometer (supplementary material, Note 2) or with the divergence/convergence of incident parallel laser beams [multi-beam optical sensor (MOS)] (supplementary material, Note 3).[38] The laser divergence method is rapid and can be used for *in situ* stress studies. By comparing stress obtained with substrate curvature [Eq. (3)] and the strain from the XRD:$\sin^2\psi$ [Eq. (2)], the Young's modulus can be expressed as

$$E_f = \sigma_{f,curv}(1 + \nu_f)\frac{d_0}{m}. \tag{4}$$

We caution that this method will introduce a considerable amount of uncertainty if low strain values are observed, and the measured stress from curvature is small.

B. Thermal strain from a CTE mismatch

After depositing perovskite films from solution, an annealing step is typically used to remove residual solvent, complete the transition from intermediate to perovskite phases, and enhance crystallinity.[39,40] Several studies have determined that high anneal
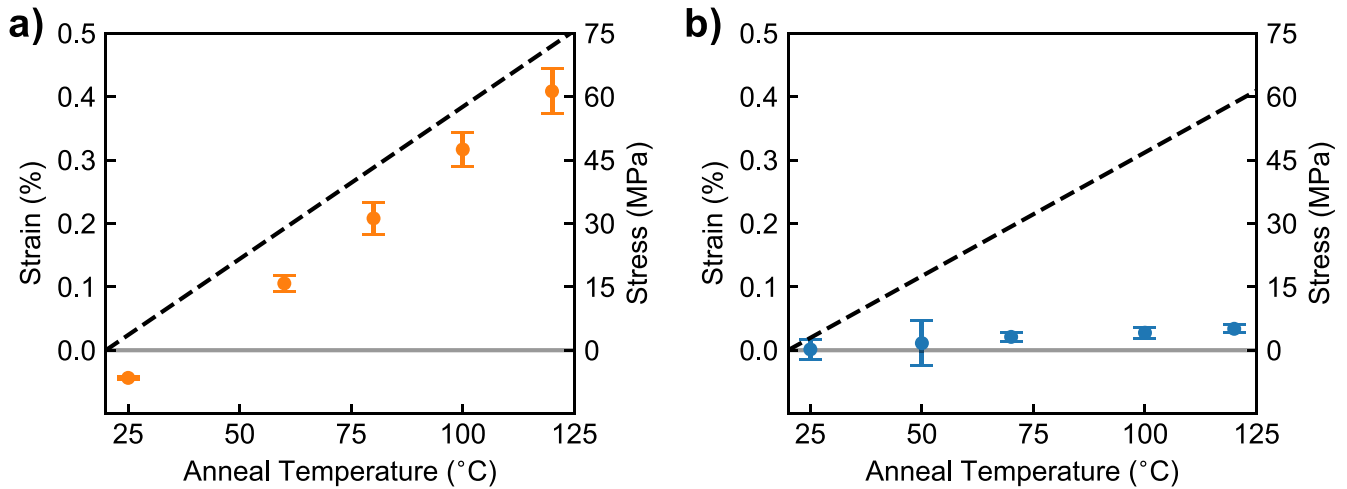
FIG. 1. Residual strain and stress in (a) SnPb ($Cs_{0.25}FA_{0.75}Sn_{0.5}Pb_{0.5}I_3$) and (b) triple cation ($Cs_{0.05}MS_{0.16}FA_{0.79}Pb$ ($I_{0.83}Br_{0.17}$)$_3$) perovskites as a function of anneal temperature. Film thickness for SnPb and triple cation perovskites shown here were 690 and 310 nm, respectively. Strain measured with XRD:$sin^2\psi$ at room temperature and stress inferred with the perovskite Young's modulus. The dashed black line represents the strain predicted by the CTE mismatch equation assuming attachment of the perovskite film to the substrate occurred at the anneal temperature [Eq. (5)]. All films were prepared on glass substrates.

temperatures (>100 °C) result in large columnar grains, superior PCEs, structural stability, and homogeneous mixing of A-site cations.[10,41–43] The CTE mismatch between a perovskite and substrates, such as glass or silicon, is predicted to contribute to in-plane biaxial tensile strain[17]

$$\varepsilon_{\Delta T} = (\alpha_s - \alpha_p)(T - T_{ref}), \quad (5)$$

where α_s and α_p are the CTEs of the substrate and the perovskite, respectively, T is the current temperature, and T_{ref} is the temperature where zero thermal strain is present. It has previously been thought that T_{ref} corresponds with the annealing temperature where complete crystallization and film formation has occurred. Following works from Zhao *et al.*[11] and Rolston *et al.*[10] stresses for solution processed perovskites have been reported from 7 to 150 MPa.[37,44,45] Although these values could be slightly inflated due to artificially high Young's moduli, little attention has been given to explain the source of variance.

Strain in SnPb ($Cs_{0.25}FA_{0.75}Sn_{0.5}Pb_{0.5}I_3$) and triple cation ($Cs_{0.05}MS_{0.16}FA_{0.79}Pb$ ($I_{0.83}Br_{0.17}$)$_3$) is shown in Fig. 1 as a function of the anneal temperature using the XRD:$sin^2\psi$ method. The SnPb composition was selected for this study due to its widespread use as the narrow bandgap layer in all-perovskite tandems,[46] whereas triple cation represents a popularized choice for efficient and stable single-junction cells.[47] Substrate curvature was used to verify the corresponding stress and Young's modulus in accordance with Eq. (4). For example, the Young's modulus for SnPb was calculated as 10.4 ± 2.2 GPa, which is at the low end of values reported using nanoindentation-based techniques for compositionally similar perovskites (Fig. S5).[34] For triple cation, the calculated Young's modulus (10.6 ± 3.9 GPa) does agree with reported values,[48] but comes with a high degree of uncertainty due to the low-strain and stress for this composition (Fig. S4). The CTEs of perovskite powders

were measured using temperature dependent XRD to avoid complications associated with the perovskite being unable to expand due to attachment to the substrate (Figs. S6–S8). The CTEs and other material properties of perovskites and substrates are summarized in Table S5.

For typical processing conditions used for high performing narrow-bandgap perovskite solar cells, we observe tension that exceeds 60 MPa [Fig. 1(a)].[46] The slope of strain vs temperature was $(4.8 ± 0.1) \times 10^{-3}\%/°C$. This slope matches that predicted from the CTE mismatch between SnPb and glass substrate $(4.8 \times 10^{-3}\%/°C)$ and indicates that film attachment to the substrate occurs at the annealing temperature. The compressive offset could be attributed to intrinsic stress factors, such as excess material inserted into grain boundaries,[49] as there is −7 MPa in films left at room temperature. For triple cation, the stress was near zero with minimal dependence on the anneal temperature [Fig. 1(b)]. The measured slope of strain vs temperature was $(3.2 ± 0.3) \times 10^{-4}\%/°C$, which is an order of magnitude lower than that predicted based on the CTE mismatch $(3.9 \times 10^{-3}\%/°C)$. These results differ from those presented by Rolston *et al.* in which triple cation on both glass and silicon had tensile stress, which increased with the anneal temperature.[10] This result supports the idea that the perovskite can attach to the substrate with a T_{ref} well below the anneal temperature without significant alterations of fabrication processes.

C. The process of mechanical attachment

Attachment to the substrate at temperatures lower than that of the anneal has been proposed to explain stress lower than predicted by the CTE mismatch.[15,50] Here, for the first time, we use a series of *in situ* characterization techniques to present direct evidence in support of this hypothesis. Although triple cation begins to crystallize prior to the anneal, as indicated by *in situ* photoluminescence, its conversion to the perovskite phase is incomplete (Fig. S11). *In situ*
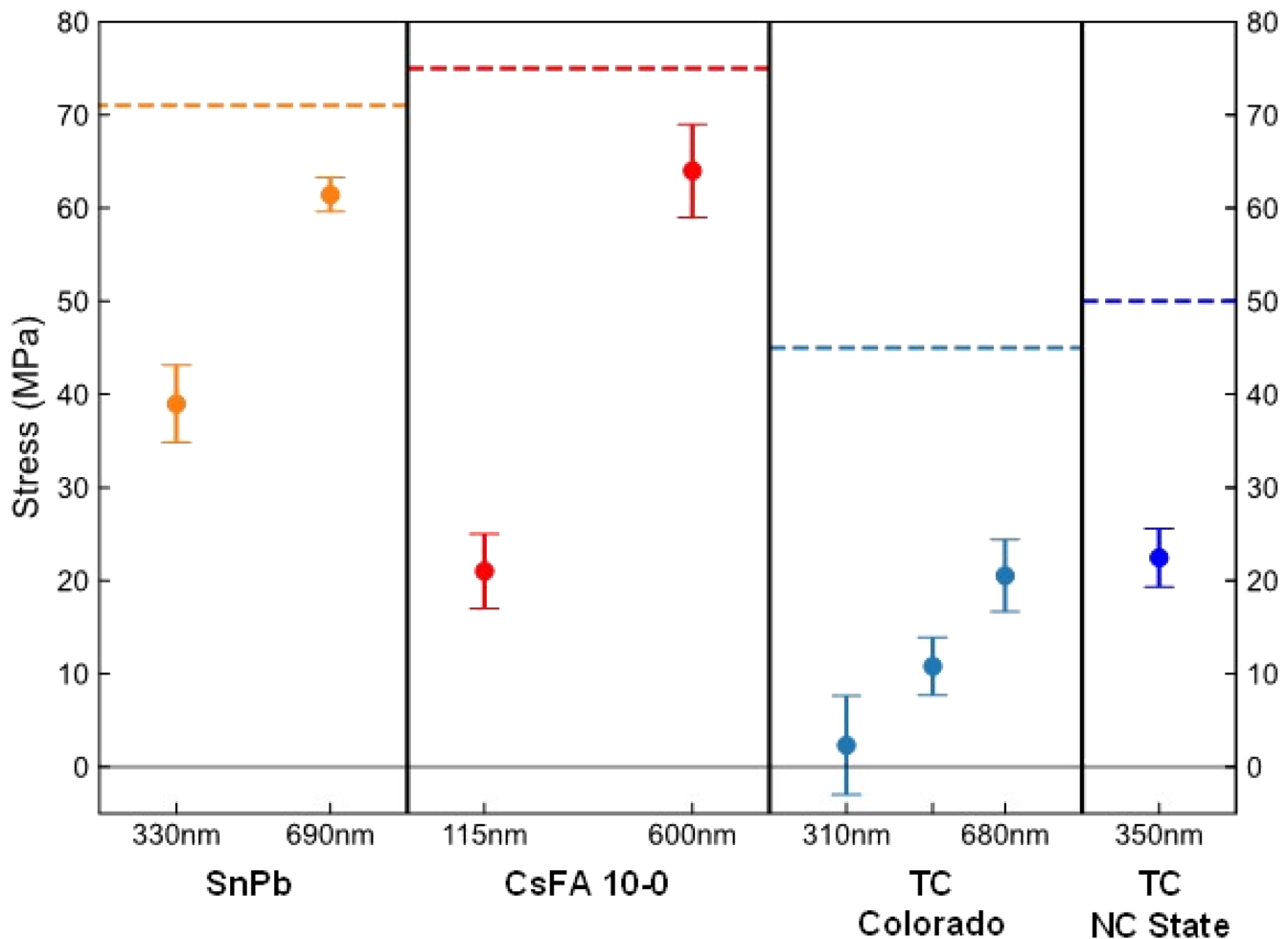
FIG. 2. Stress vs post anneal film thickness for SnPb (orange), CsFA 10-0 (red), triple cation (TC) spun at Colorado (light blue), and TC spun at NC State (blue). For SnPb and TC, strain was measured using the XRD:$\sin^2\psi$ method and stress inferred with a calculated Young's Modulus [Eq. (4)]. For CsFA 10-0, stress was directly inferred from the substrate curvature method [Eq. (3)]. The colored dashed lines represent the strain predicted by the CTE mismatch equation [Eq. (5)]. SnPb and TC spun at Colorado were deposited on glass while CsFA 10-0 and TC spun at NC State were deposited on silicon.

ultraviolet-visible (UV–vis) absorbance measurements indicate that only 60% of the eventual thickness has converted prior to the anneal (Fig. S12). Also, solution processed perovskites have been shown to nucleate crystallites at the top interface followed by growth toward the substrate [Fig. 3(d)].[51] So, the definition of attachment to the substrate is not synonymous with complete film formation, removal of solvent complexes, or conversion to the eventual cubic, α-phase perovskite.

To control the converted fraction of perovskite prior to the anneal we varied the film thickness of SnPb, CsFA10-0 ($Cs_{0.1}FA_{0.9}PbI_3$), and triple cation and measured residual strain [Fig. 2]. For all compositions studied here, the strain increases with film thickness. Interestingly, all strain values were below that predicted by the CTE mismatch equation [Eq. (5)], which suggests some level of attachment prior to the anneal or the presence of intrinsic strain contributions.[52] In contrast with triple cation film prepared

at the University of Colorado–Boulder, identically prepared triple cation films at NC State that were shipped to and measured in Colorado exhibit significantly higher strain. Lab-to-lab variation in this study and compared with previous reports[10] could be explained by a difference in processing environments, such as barometric pressure, which influences solvent evaporation and corresponding crystallization kinetics.[53] The barometric pressure in Boulder is 0.83 atm, while that at NC State and Stanford is ~1 atm.

To better understand the deviation of stress from the CTE mismatch equation and the dependence on final film thickness, we conducted *in situ* stress measurements using a laser deflection system (MOS) during the anneal and subsequent cooldown of CsFA 10-0 [Figs. 3(a) and 3(b)]. Previous depictions of residual stress in perovskites would predict the stress to be near zero at the anneal temperature where complete film formation and mechanical attachment to the substrate occur. Consequently, T_{ref} in Eq. (5) would
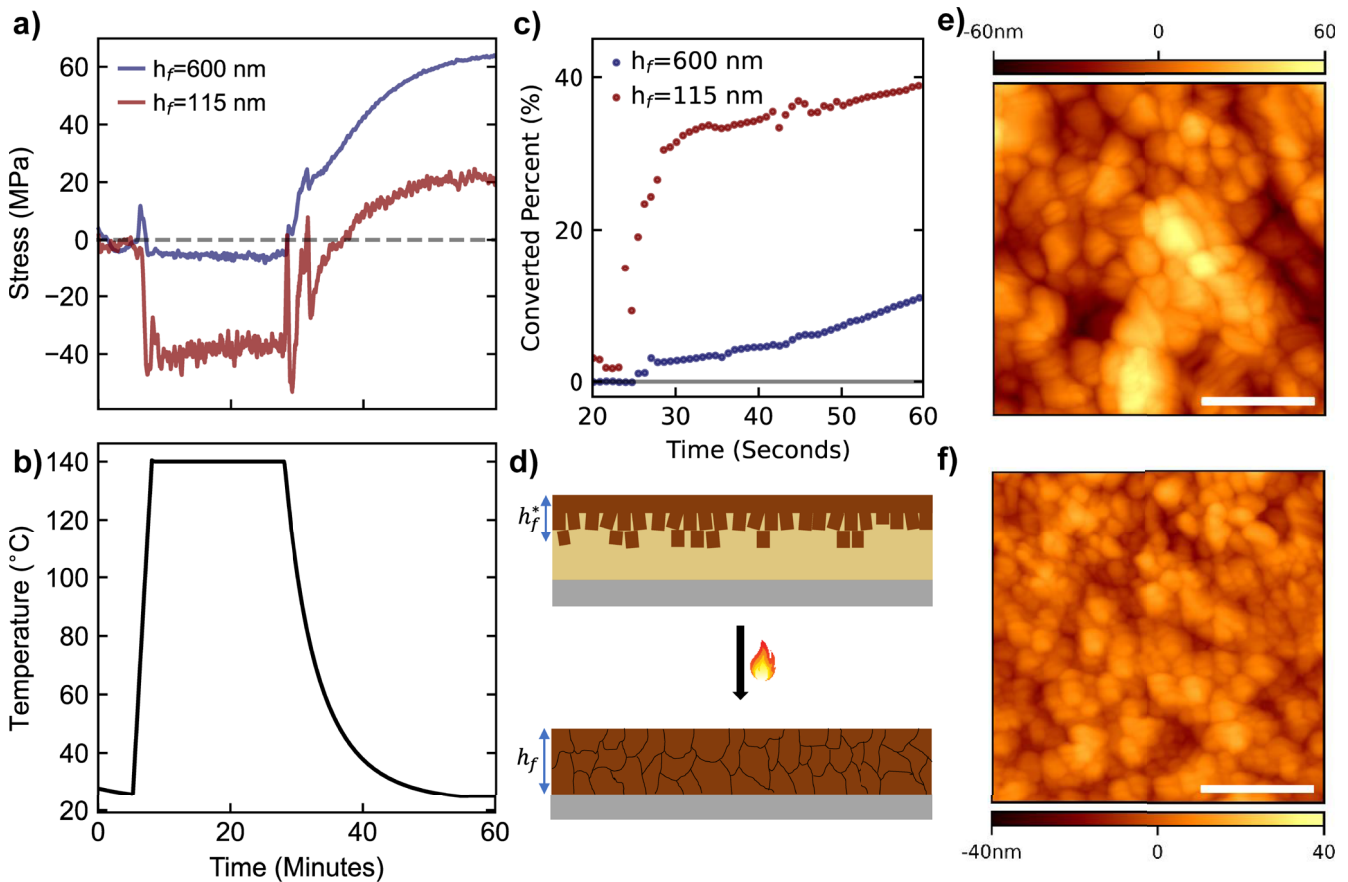
FIG. 3. For CsFA 10-0 perovskite: (a) Stress measured with laser substrate curvature vs time during the anneal and cooldown procedure where h_f represents the post anneal film thickness. Films were annealed in argon on silicon substrates, (b) corresponding temperature profile of the anneal and cooldown, (c) converted thickness percent vs time during spin coating from *in situ* UV–vis absorbance, (d) schematic of top-down crystallization and growth of solution processed perovskites, (e) Atomic Force Microscopy (AFM) topography image for CsFA 10-0 with final film thickness of 600 nm (scale bar is 1 μm), and (f) AFM topography image for CsFA 10-0 with final film thickness of 115 nm (scale bar is 1 μm).

be this temperature. Tension would be expected to build up during the subsequent cooldown due to the CTE mismatch. The stress in the thick (600 nm) perovskite film follows this idea closely [Fig. 3(a)]. On the other hand, the thin (115 nm) perovskite film deviates significantly and is driven into compression during the temperature ramp to the eventual stabilization at the anneal temperature. Although conversion to the perovskite phase is incomplete, the compression can be explained by a top layer of perovskite mechanically attached to the substrate, which is unable to expand with its intrinsic CTE. The stress change during cooldown is comparable for both thickness conditions ($\approx$65 MPa), but T_{ref} varies by $\approx$80 °C [Eq. (5)].

In situ UV–vis absorbance was conducted to determine the thickness of converted perovskite during spin coating vs time as shown in Fig. 3(c) (Fig. S13). The film with the higher converted percentage (40%) prior to the anneal has a higher degree of attachment and a resulting lower residual stress after cooldown as there

is less solution to convert. This relationship was also observed for triple cation perovskite in which converted percentages of 60% and 73% correspond with residual stress difference of $\approx$16 MPa (Fig. S12). Varying thickness provided a straightforward way to demonstrate that a degree of attachment prior to the anneal is a way to reduce residual stress in perovskites. However, we acknowledge that due to light absorption constraints, thinning the perovskite layer is not an ideal strategy for solar cells. In addition, although driving conversion prior to anneal can be a means to avoid residual tensile stress, we show below that conversion does not universally guarantee permanent attachment to the substrate.

We show in the supplementary material, Note 3, that SnPb films exhibit enhanced stability under applied uniaxial compression upon aging under 85 °C in an ambient environment (relative humidity $\approx$20%). Reducing the annealing temperature has been proposed as a strategy to avoid tension driven by the CTE mismatch
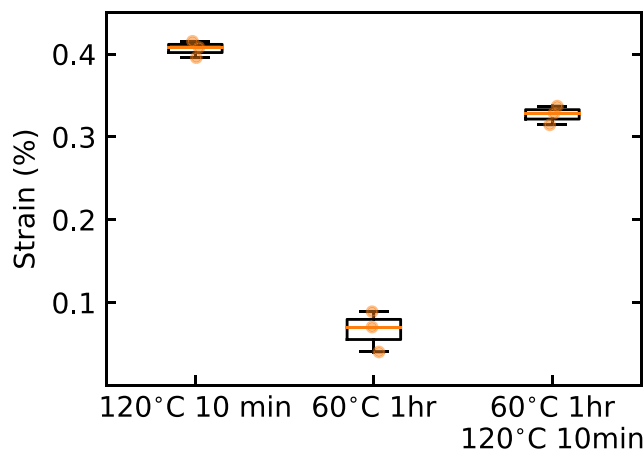
FIG. 4. Strain measured with the XRD:sin²ψ for SnPb perovskite for standard (120 °C for 10 min), reduced (60 °C for 1 h), and two-step (60 °C for 1 h followed by 120 °C for 10 min) annealing conditions. Films had film thickness of 690 nm and were deposited on glass substrates.

between substrate and perovskite.[10] Therefore, we hypothesized that it could be beneficial to use a lower annealing temperature to drive the attachment process for SnPb followed by an elevated anneal temperature to enhance crystallinity and cation homogeneity.[42] A two-step anneal was conducted in which the film was annealed at 60 °C for 1 h, cooled to room temperature, and followed by an anneal at 120 °C for 10 min. While there is tension after cooling from the 60 °C anneal, indicating thermal strain, the strain increases by 0.26% after re-annealing at the elevated temperature (Fig. 4). We speculate that this increase in strain can be explained by reformation at the substrate interface that resets the reference temperature [Eq. (5)]. This phenomenon was not observed for the other perovskite compositions studied (triple cation and CsFA10-0). Perovskites are known to be visco-plastic at high stresses experienced during nanoindentation[54] and probably exhibit a degree of visco-elasticity at these lower stresses. The soft and visco-elastic properties of the perovskites combined with the elevated temperature, grain growth (from 87 to 176 nm), and compression ($\varepsilon \approx -0.48\%$) that occur at the 120 °C anneal step probably enable interfacial slippage (Fig. S14, supplementary material, Note 6).[34]

III. CONCLUSION

In summary, we have identified stress in perovskite films that is dependent on composition and deviates from prediction based on the CTE mismatch with the substrate. The relationship between strain and anneal temperature reveals that it is possible to attach a perovskite film to the substrate without complete perovskite formation. By monitoring stress during the anneal and cooldown, we provide direct evidence that the mechanical attachment can occur prior to the anneal for solution processed perovskites. However, we also show that certain perovskite compositions exhibit impermanent attachment despite high degrees of film formation. The dynamic process of mechanical attachment

to the substrate observed in this work provides insights into the deviation of stress from a simple application of the CTE mismatch equation and varying stresses reported in literature. This emphasizes the importance of mechanical stress measurements as it influences stability, reliability, and durability, which are critical for perovskite solar cells to contribute to aggressive renewable energy goals.

SUPPLEMENTARY MATERIAL

Experimental details, XRD strain measurements, substrate curvature, *in situ* photoluminescence spectra, *in situ* UV–vis absorption spectra, temperature dependent XRD results, perovskite aging study results, and material parameters used for models and calculations can be found in the supplementary material.

AUTHOR DECLARATIONS

Conflict of Interests

McGehee is an advisor to Swift Solar.

Author Contributions

Gabriel R. McAndrews: Conceptualization (lead); Investigation (lead); Methodology (lead); Validation (lead); Writing – original draft (lead); Writing – review & editing (lead). **Boyu Guo**: Conceptualization (supporting); Investigation (supporting); Validation (supporting); Writing – review & editing (supporting). **Daniel A. Morales**: Investigation (supporting); Validation (supporting). **Aram Amassian**: Conceptualization (equal); Project administration (equal); Supervision (equal); Writing – review & editing (equal). **Michael D. McGehee**: Conceptualization (equal); Project administration (equal); Supervision (equal); Writing – review & editing (equal).

DATA AVAILABILITY

The data that support the findings of this study are available within the article and its supplementary material.

REFERENCES

[1] K. Yoshikawa, H. Kawasaki, W. Yoshida, T. Irie, K. Konishi, K. Nakano, T. Uto, D. Adachi, M. Kanematsu, H. Uzu, and K. Yamamoto, "Silicon heterojunction solar cell with interdigitated back contacts for a photoconversion efficiency over 26%," Nat. Energy **2**(5), 17032 (2017).

[2] Best Research-Cell Efficiency Chart.

[3] KAUST Team Sets World Record for Tandem Solar Cell Efficiency, 2023.

[4] J. A. Christians, P. A. Miranda Herrera, and P. V. Kamat, "Transformation of the excited state and photovoltaic efficiency of $CH_3NH_3PbI_3$ perovskite upon controlled exposure to humidified air," J. Am. Chem. Soc. **137**(4), 1530–1538 (2015).

[5] Y. Ouyang, Y. Li, P. Zhu, Q. Li, Y. Gao, J. Tong, L. Shi, Q. Zhou, C. Ling, Q. Chen, Z. Deng, H. Tan, W. Deng, and J. Wang, "Photo-oxidative degradation of methylammonium lead iodide perovskite: Mechanism and protection," J. Mater. Chem. A **7**(5), 2275–2282 (2019).

[6] A. Kumar, U. Bansode, S. Ogale, and A. Rahman, "Understanding the thermal degradation mechanism of perovskite solar cells via dielectric and noise measurements," Nanotechnology **31**(36), 365403 (2020).

[7] J. S. Yun, J. Kim, T. Young, R. J. Patterson, D. Kim, J. Seidel, S. Lim, M. A. Green, S. Huang, and A. Ho-Baillie, "Humidity-induced degradation via grain boundaries of $HC(NH_2)_2PbI_3$ planar perovskite solar cells," Adv. Funct. Mater. **28**(11), 1705363 (2018).

[8] C. C. Boyd, R. Cheacharoen, T. Leijtens, and M. D. McGehee, "Understanding degradation mechanisms and improving stability of perovskite photovoltaics," Chem. Rev. **119**(5), 3418–3451 (2019).

[9] X. Zhao, T. Liu, Q. C. Burlingame, T. Liu, R. Holley, G. Cheng, N. Yao, F. Gao, and Y.-L. Loo, "Accelerated aging of all-inorganic, interface-stabilized perovskite solar cells," Science **377**(6603), 307–310 (2022).

[10] N. Rolston, K. A. Bush, A. D. Printz, A. Gold-Parker, Y. Ding, M. F. Toney, M. D. McGehee, and R. H. Dauskardt, "Engineering stress in perovskite solar cells to improve stability," Adv. Energy Mater. **8**(29), 1802139 (2018).

[11] J. Zhao, Y. Deng, H. Wei, X. Zheng, Z. Yu, Y. Shao, J. E. Shield, and J. Huang, "Strained hybrid perovskite thin films and their impact on the intrinsic stability of perovskite solar cells," Sci. Adv. **3**(11), eaao5616 (2017).

[12] L. A. Muscarella, E. M. Hutter, F. Wittmann, Y. W. Woo, Y.-K. Jung, L. McGovern, J. Versluis, A. Walsh, H. J. Bakker, and B. Ehrler, "Lattice compression increases the activation barrier for phase segregation in mixed-halide perovskites," ACS Energy Lett. **5**(10), 3152–3158 (2020).

[13] Y. Zhao, P. Miao, J. Elia, H. Hu, X. Wang, T. Heumueller, Y. Hou, G. J. Matt, A. Osvet, Y.-T. Chen, M. Tarragó, D. de Ligny, T. Przybilla, P. Denninger, J. Will, J. Zhang, X. Tang, N. Li, C. He, A. Pan, A. J. Meixner, E. Spiecker, D. Zhang, and C. J. Brabec, "Strain-activated light-induced halide segregation in mixed-halide perovskite solids," Nat. Commun. **11**(1), 6328 (2020).

[14] T. Haeger, R. Heiderhoff, and T. Riedl, "Thermal properties of metal-halide perovskites," J. Mater. Chem. C **8**(41), 14289–14311 (2020).

[15] C. Ramirez, S. K. Yadavalli, H. F. Garces, Y. Zhou, and N. P. Padture, "Thermomechanical behavior of organic-inorganic halide perovskites for solar cells," Scr. Mater. **150**, 36–41 (2018).

[16] T. W. Jones, A. Osherov, M. Alsari, M. Sponseller, B. C. Duck, Y.-K. Jung, C. Settens, F. Niroui, R. Brenes, C. V. Stan, Y. Li, M. Abdi-Jalebi, N. Tamura, J. Emyr Macdonald, M. Burghammer, R. H. Friend, V. Bulović, A. Walsh, G. J. Wilson, S. Lilliu, and S. D. Stranks, "Lattice strain causes non-radiative losses in halide perovskites," Energy Environ. Sci. **12**(2), 596–606 (2019).

[17] L. B. Freund and S. Suresh, *Thin Film Materials: Stress, Defect Formation and Surface Evolution* (Cambridge University Press, Cambridge, 2004).

[18] N. Rolston, A. D. Printz, J. M. Tracy, H. C. Weerasinghe, D. Vak, L. J. Haur, A. Priyadarshi, N. Mathews, D. J. Slotcavage, M. D. McGehee, R. E. Kalan, K. Zielinski, R. L. Grimm, H. Tsai, W. Nie, A. D. Mohite, S. Gholipour, M. Saliba, M. Grätzel, and R. H. Dauskardt, "Effect of cation composition on the mechanical stability of perovskite solar cells," Adv. Energy Mater. **8**(9), 1702116 (2018).

[19] N. Rolston, B. L. Watson, C. D. Bailie, M. D. McGehee, J. P. Bastos, R. Gehlhaar, J.-E. Kim, D. Vak, A. T. Mallajosyula, G. Gupta, A. D. Mohite, and R. H. Dauskardt, "Mechanical integrity of solution-processed perovskite solar cells," Extreme Mech. Lett. **9**, 353–358 (2016).

[20] B. L. Watson, N. Rolston, A. D. Printz, and R. H. Dauskardt, "Scaffold-reinforced perovskite compound solar cells," Energy Environ. Sci. **10**(12), 2500–2508 (2017).

[21] M. Gutwald, N. Rolston, A. D. Printz, O. Zhao, H. Elmaraghi, Y. Ding, J. Zhang, and R. H. Dauskardt, "Perspectives on intrinsic toughening strategies and passivation of perovskite films with organic additives," Sol. Energy Mater. Sol. Cells **209**, 110433 (2020).

[22] A. Giuri, N. Rolston, S. Colella, A. Listorti, C. Esposito Corcione, H. Elmaraghi, S. Lauciello, R. H. Dauskardt, and A. Rizzo, "Robust, high-performing maize–perovskite-based solar cells with improved stability," ACS Appl. Energy Mater. **4**(10), 11194–11203 (2021).

[23] R. Cheacharoen, N. Rolston, D. Harwood, K. A. Bush, R. H. Dauskardt, and M. D. McGehee, "Design and understanding of encapsulated perovskite solar cells to withstand temperature cycling," Energy Environ. Sci. **11**(1), 144–150 (2018).

[24] M. Dailey, Y. Li, and A. D. Printz, "Residual film stresses in perovskite solar cells: Origins, effects, and mitigation strategies," ACS Omega **6**(45), 30214–30223 (2021).

[25] D. Liu, D. Luo, A. N. Iqbal, K. W. P. Orr, T. A. S. Doherty, Z.-H. Lu, S. D. Stranks, and W. Zhang, "Strain analysis and engineering in halide perovskite photovoltaics," Nat. Mater. **20**(10), 1337–1346 (2021).

[26] E. G. Moloney, V. Yeddu, and M. I. Saidaminov, "Strain engineering in halide perovskites," ACS Mater. Lett. **2**(11), 1495–1508 (2020).

[27] B. Jin, J. Cao, R. Yuan, B. Cai, C. Wu, and X. Zheng, "Strain relaxation for perovskite lattice reconfiguration," Adv. Energy Sustainability Res. **4**(4), 2200143 (2023).

[28] Q. Luo and A. H. Jones, "High-precision determination of residual stress of polycrystalline coatings using optimised XRD-$sin^2\psi$ technique," Surf. Coat. Technol. **205**(5), 1403–1408 (2010).

[29] V. Hauk, in *Structural and Residual Stress Analysis by Nondestructive Methods*, edited by V. Hauk (Elsevier Science B.V., Amsterdam, 1997), pp. 17–65.

[30] A. Wyss, A. S. Sologubenko, N. Mishra, P. A. Gruber, and R. Spolenak, "Monitoring of stress–strain evolution in thin films by reflection anisotropy spectroscopy and synchrotron x-ray diffraction," J. Mater. Sci. **52**(11), 6741–6753 (2017).

[31] C. L. Azanza Ricardo, G. Degan, M. Bandini, and P. Scardi, "Residual stress depth-profiling in shot-peened Al alloy components subjected to fatigue testing," Mater. Sci. Forum **638-642**, 2464–2469 (2010).

[32] L. Wang, Q. Song, F. Pei, Y. Chen, J. Dou, H. Wang, C. Shi, X. Zhang, R. Fan, W. Zhou, Z. Qiu, J. Kang, X. Wang, A. Lambertz, M. Sun, X. Niu, Y. Ma, C. Zhu, H. Zhou, J. Hong, Y. Bai, W. Duan, K. Ding, and Q. Chen, "Strain modulation for light-stable n-i-p perovskite/silicon tandem solar cells," Adv. Mater. **34**(26), 2201315 (2022).

[33] J. Feng, "Mechanical properties of hybrid organic-inorganic $CH_3NH_3BX_3$ (B = Sn, Pb; X = Br, I) perovskites for solar cell absorbers," APL Mater. **2**(8), 081801 (2014).

[34] Q. Tu, D. Kim, M. Shyikh, and M. G. Kanatzidis, "Mechanics-coupled stability of metal-halide perovskites," Matter **4**(9), 2765–2809 (2021).

[35] M. Layek, I. Yang, Z. Dai, A. Ranka, T. Cai, B. W. Sheldon, E. Chason, and N. P. Padture, "Elastic modulus of polycrystalline halide perovskite thin films on substrates," arXiv:230707.07071 (2023).

[36] G. G. Stoney, "The tension of metallic films deposited by electrolysis," Proc. R. Soc. A **82**(553), 172–175 (1909).

[37] H. Wang, C. Zhu, L. Liu, S. Ma, P. Liu, J. Wu, C. Shi, Q. Du, Y. Hao, S. Xiang, H. Chen, P. Chen, Y. Bai, H. Zhou, Y. Li, and Q. Chen, "Interfacial residual stress relaxation in perovskite solar cells with improved stability," Adv. Mater. **31**(48), 1904408 (2019).

[38] E. Chason and J. A. Floro, "Measurements of stress evolution during thin film deposition," MRS Proc. **428**, 499 (1996).

[39] A. D. Taylor, Q. Sun, K. P. Goetz, Q. An, T. Schramm, Y. Hofstetter, M. Litterst, F. Paulus, and Y. Vaynzof, "A general approach to high-efficiency perovskite solar cells by any antisolvent," Nat. Commun. **12**(1), 1878 (2021).

[40] Z. Saki, M. M. Byranvand, N. Taghavinia, M. Kedia, and M. Saliba, "Solution-processed perovskite thin-films: The journey from lab- to large-scale solar cells," Energy Environ. Sci. **14**(11), 5690–5722 (2021).

[41] X. Cao, L. Zhi, Y. Jia, Y. Li, X. Cui, K. Zhao, L. Ci, K. Ding, and J. Wei, "High annealing temperature induced rapid grain coarsening for efficient perovskite solar cells," J. Colloid Interface Sci. **524**, 483–489 (2018).

[42] L. E. Mundt, F. Zhang, A. F. Palmstrom, J. Xu, R. Tirawat, L. L. Kelly, K. H. Stone, K. Zhu, J. J. Berry, M. F. Toney, and L. T. Schelhas, "Mixing matters: Nanoscale heterogeneity and stability in metal halide perovskite solar cells," ACS Energy Lett. **7**, 471–480 (2021).

[43] L. T. Schelhas, Z. Li, J. A. Christians, A. Goyal, P. Kairys, S. P. Harvey, D. H. Kim, K. H. Stone, J. M. Luther, K. Zhu, V. Stevanovic, and J. J. Berry, "Insights into operational stability and processing of halide perovskite active layers," Energy Environ. Sci. **12**(4), 1341–1348 (2019).

[44] C. Shi, Q. Song, H. Wang, S. Ma, C. Wang, X. Zhang, J. Dou, T. Song, P. Chen, H. Zhou, Y. Chen, C. Zhu, Y. Bai, and Q. Chen, "Molecular hinges stabilize formamidinium-based perovskite solar cells with compressive strain," Adv. Funct. Mater. **32**(28), 2201193 (2022).

[45] D.-J. Xue, Y. Hou, S.-C. Liu, M. Wei, B. Chen, Z. Huang, Z. Li, B. Sun, A. H. Proppe, Y. Dong, M. I. Saidaminov, S. O. Kelley, J.-S. Hu, and E. H. Sargent, "Regulating strain in perovskite thin films through charge-transport layers," Nat. Commun. **11**(1), 1514 (2020).

[46] J. Werner, T. Moot, T. A. Gossett, I. E. Gould, A. F. Palmstrom, E. J. Wolf, C. C. Boyd, M. F. A. M. van Hest, J. M. Luther, J. J. Berry, and M. D. McGehee, "Improving low-bandgap tin–lead perovskite solar cells via contact engineering and gas quench processing," ACS Energy Lett. **5**(4), 1215–1223 (2020).

[47] M. Saliba, T. Matsui, J.-Y. Seo, K. Domanski, J.-P. Correa-Baena, M. K. Nazeeruddin, S. M. Zakeeruddin, W. Tress, A. Abate, A. Hagfeldt, and M. Grätzel, "Cesium-containing triple cation perovskite solar cells: Improved stability, reproducibility and high efficiency," Energy Environ. Sci. **9**(6), 1989–1997 (2016).

[48] I. Mela, C. Poudel, M. Anaya, G. Delport, K. Frohna, S. Macpherson, T. A. S. Doherty, A. Scheeder, S. D. Stranks, and C. F. Kaminski, "Revealing nanomechanical domains and their transient behavior in mixed-halide perovskite films," Adv. Funct. Mater. **31**(23), 2100293 (2021).

[49] Y. Sun, Q. Yao, W. Xing, H. Jiang, Y. Li, W. Xiong, W. Zhu, and Y. Zheng, "Residual strain evolution induced by crystallization kinetics during anti-solvent spin coating in organic–inorganic hybrid perovskite," Adv. Sci. **10**(18), 2205986 (2023).

[50] J. Tong, J. Gong, M. Hu, S. K. Yadavalli, Z. Dai, F. Zhang, C. Xiao, J. Hao, M. Yang, M. A. Anderson, E. L. Ratcliff, J. J. Berry, N. P. Padture, Y. Zhou, and K. Zhu, "High-performance methylammonium-free ideal-band-gap perovskite solar cells," Matter **4**(4), 1365–1376 (2021).

[51] S. Chen, X. Xiao, B. Chen, L. L. Kelly, J. Zhao, Y. Lin, M. F. Toney, and J. Huang, "Crystallization in one-step solution deposition of perovskite films: Upward or downward?," Sci. Adv. **7**(4), eabb2412 (2021).

[52] G. Abadias, E. Chason, J. Keckes, M. Sebastiani, G. B. Thompson, E. Barthel, G. L. Doll, C. E. Murray, C. H. Stoessel, and L. Martinu, "Review article: Stress in thin films and coatings: Current status, challenges, and prospects," J. Vac. Sci. Technol. A **36**(2), 020801 (2018).

[53] *Handbook of Solvents*, edited by G. Wypych, 2nd ed. (ChemTec Publishing, Oxford, 2014), pp. 11–72

[54] M. A. Reyes-Martinez, A. L. Abdelhady, M. I. Saidaminov, D. Y. Chung, O. M. Bakr, M. G. Kanatzidis, W. O. Soboyejo, and Y.-L. Loo, "Time-dependent mechanical response of APbX$_3$ (A = Cs, CH$_3$NH$_3$; X = I, Br) single crystals," Adv. Mater. **29**(24), 1606556 (2017).